Protein Science (1994), *3*:227-239. Cambridge University Press. Printed in the USA.

Role of the Cys 2–Cys 10 disulfide bond for the structure, stability, and folding kinetics of ribonuclease T1

LORENZ M. MAYR,[1,4] DIETER WILLBOLD,[2] OLFERT LANDT,[3] AND FRANZ X. SCHMID[1]

[1] Lehrstuhl für Biochemie, Universität Bayreuth, Universitätsstr. 30, D-95440 Bayreuth, Germany
[2] Lehrstuhl für Biopolymere, Universität Bayreuth, Universitätsstr. 30, D-95440 Bayreuth, Germany
[3] Institut für Kristallographie, Abteilung Saenger, Freie Universität Berlin, Takustr. 6, D-14195 Berlin, Germany

(RECEIVED August 31, 1993; ACCEPTED October 25, 1993)

Abstract

The Cys 2–Cys 10 disulfide bond in ribonuclease T1 was broken by substituting Cys 2 and Cys 10 by Ser and Asn, respectively, as present in ribonuclease F1. This C2S/C10N variant resembles the wild-type protein in structure and in catalytic activity. Minor structural changes were observed by 2-dimensional NMR in the local environment of the substituted amino acids only. The thermodynamic stability of ribonuclease T1 is strongly reduced by breaking the Cys 2–Cys 10 bond, and the free energy of denaturation is decreased by about 10 kJ/mol. The folding mechanism is not affected, and the *trans* to *cis* isomerizations of Pro 39 and Pro 55 are still the rate-limiting steps of the folding process. The differences in the time courses of unfolding and refolding are correlated with the decrease in stability: the folding kinetics of the wild-type protein and the C2S/C10N variant become indistinguishable when they are compared under conditions of identical stability. Apparently, the Cys 2–Cys 10 disulfide bond is important for the stability but not for the folding mechanism of ribonuclease T1. The breaking of this bond has the same effect on stability and folding kinetics as adding 1 M guanidinium chloride to the wild-type protein.

Keywords: disulfide bond substitution; folding kinetics; NMR; prolyl *cis/trans* isomerization; prolyl isomerase; protein folding; protein stability

Disulfide bonds are common intramolecular crosslinks in proteins that contribute substantially to the free energy of stabilization. The reversibility of protein unfolding in vitro is generally good when the disulfides are left intact in the denatured molecules, and therefore small single-domain proteins with disulfides have frequently been used to investigate the mechanism of protein folding. Such proteins include ribonucleases A and T1, lysozyme, α-lactalbumin, bovine pancreatic trypsin inhibitor, and the immunoglobulin domains (Jaenicke, 1991; Baldwin, 1993; Matthews, 1993; Roder & Elöve, 1993).

In protein folding, secondary structure is thought to form very early, followed by tertiary interactions (Gō, 1983; Roder et al., 1988; Udgaonkar & Baldwin, 1988; Radford et al., 1992), which are involved in various stages of folding. In early steps they guide the selective docking of elements of secondary structure, and in late steps they determine the correct assembly of the final native conformation. It is not clear at present whether only nativelike tertiary interactions occur during folding or whether transient nonnative contacts are important as well. Disulfide bonds can be regarded as tertiary interactions that remain covalently fixed once they are formed. During the in vitro folding of protein chains with intact disulfides, such nativelike tertiary interactions are present already in the unfolded protein and throughout the folding process. This premature fixing of tertiary interactions by intact disulfide bonds could affect the folding mechanism, e.g., by changing the order of individual steps or by favoring particular pathways.

Reprint requests to: Franz X. Schmid, Lehrstuhl für Biochemie, Universität Bayreuth, Universitätsstr. 30, D-95440 Bayreuth, Germany.

Abbreviations: RNase T1, ribonuclease T1; C2S/C10N-RNase T1, variant of ribonuclease T1 with substitution of the 2–10 disulfide bond by a serine and an asparagine residue, respectively; (2–10)-RCM-RNase T1, ribonuclease T1 with the 2–10 disulfide bond reduced and the cysteine residues carboxymethylated; PPI, peptidyl–prolyl *cis/trans* isomerase; PU, activity units for isomerization of a proline-containing peptide by PPI; GpC, guanylyl(3′-5′)cytidine; GdmCl, guanidinium chloride; NaAc, sodium acetate/acetic acid; NaOx, sodium oxalate/oxalic acid; Tris, Tris-(hydroxymethyl)-aminomethane/HCl; MES, 2-(*N*-morpholino)-ethanesulfonic acid/HCl; PIPES, piperazine-*N*,*N*′-bis(ethanesulfonic acid)/HCl; U_F, fast-folding species; U_S, slow-folding species; DQF-COSY, double quantum filtered correlated spectroscopy; TOCSY, total correlated spectroscopy; NOESY, NOE spectroscopy; $\Delta G_D^{H_2O}$, Gibbs free energy of denaturation in the absence of denaturant; $m = d\Delta G_D/d[\text{GdmCl}]$. We use the terms *cis* proline or *trans* proline for proline residues that are preceded by a *cis* or a *trans* peptide bond, respectively.

[4]Present address: Whitehead Institute, MIT, 9 Cambridge Center, Cambridge, Massachusetts 02142.

To investigate the role of a disulfide for the folding mechanism we use RNase T1 as a model and compare the folding kinetics of the wild-type protein with the folding of a variant that lacks one of the 2 disulfide bonds. We use RNase T1 because the folding kinetics of this protein with both disulfides intact are well characterized. RNase T1 is a small, single-domain protein of 104 amino acids (M_r = 11,085 Da) with an extended α-helix of 4.5 turns and 2 antiparallel β-sheets (Heinemann & Saenger, 1982; Martinez-Oyanedel et al., 1991). The 2 disulfide bonds are spatially close to each other in the folded protein (Fig. 1A). The C2–C10 bond connects 2 successive β-strands near the amino-terminus of the RNase T1 chain; it is about 90% accessible to solvent and can be selectively reduced by dithiothreitol (Pace & Creighton, 1986; Pace et al., 1988). The C6–C103 disulfide links the amino- and the carboxy-terminal regions of the RNase T1 chain and is inaccessible to solvent.

During the refolding of RNase T1 with intact disulfides, partially folded intermediates with extensive secondary structure and some tertiary interactions accumulate rapidly at early stages (Kiefhaber et al., 1992c; Mullins et al., 1993). The final slow steps of folding are limited in rate by the *trans* to *cis* isomerizations of the prolyl peptide bonds at Pro 39 and Pro 55 (Kiefhaber et al., 1990b, 1990c; Mayr & Schmid, 1993b). Acquisition of ordered structure and prolyl isomerizations are interrelated processes. In particular, the *trans* to *cis* isomerization at Pro 39 is decelerated by the rapid formation of compact structure. Both Pro 39 and Pro 55 are distant from the C2–C10 disulfide bond in the folded protein (cf. Fig. 1A).

The C2–C10 disulfide bond is not conserved in evolution, and Cys 2 is replaced by a serine and Cys 10 by an asparagine in RNase F1 (Fig. 1B). The same replacements were used here to disrupt the C2–C10 bond of RNase T1 by protein engineering. In our experiments we examine first the consequences of these mutations for the structure, the activity, and the stability of RNase T1. Then we characterize the kinetics of unfolding and refolding of the C2S/C10N variant under various conditions and its catalysis by prolyl isomerase in comparison to the wild-type protein.

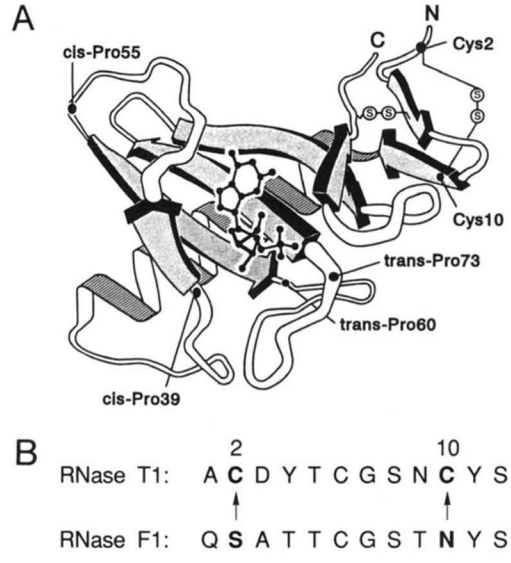

Fig. 1. A: Schematic drawing of the backbone conformation of RNase T1. The positions of *cis* prolines 39 and 55, *trans* prolines 60 and 73, and the Cys 2–Cys 10 disulfide bond are indicated. (Drawing courtesy of Dr. U. Heinemann, Berlin, with bound 2′-GMP as a substrate.) **B:** Amino acid sequences of RNase T1 and RNase F1.

Results

Enzymatic activity of C2S/C10N-RNase T1

The breaking of the C2–C10 disulfide bond left the enzymatic activity of RNase T1 almost unchanged. The relative activities of the wild-type protein and the C2S/C10N variant toward the dinucleotide GpC and toward yeast RNA are compared in Table 1. The results for wild-type RNase T1 are in good agreement with the data of Zabinski and Walz (1976). Both K_m and k_{cat} for GpC are almost unaffected by the C2S/C10N mutation, and the value of k_{cat}/K_m is decreased from 100% to 88%. With RNA as a substrate, the relative activity is decreased to 81%. A similar decrease to 86% was reported under slightly different conditions for (2–10)-RCM-RNase T1, where the C2–C10 disulfide bond was chemically reduced and carboxymethylated (Pace et al., 1988).

Circular dichroism spectra of C2S/C10N-RNase T1

The structural consequences of the disruption of the C2–C10 disulfide bond were investigated by CD spectroscopy and by 2D-NMR. The C2S/C10N mutation leads to changes in the CD spectra in the far UV (Fig. 2A) and near UV regions (Fig. 2B). Between 190 and 250 nm the CD spectrum is very similar in

Table 1. *Steady-state kinetic parameters of wild-type RNase T1 and the C2S/C10N variant*[a]

Substrate	Variant	K_M (μM)	k_{cat} (s^{-1})	k_{cat}/K_M ($mM^{-1}\ s^{-1}$)	Spec. act. (ΔOD/min * mg)	Rel. act. (%)
RNA	Wild type	–	–	–	58.2	100
RNA	C2S/C10N	–	–	–	48.31	81.5
GpC	Wild type	129 ± 7	249 ± 6	1,930 ± 143	–	100
GpC	C2S/C10N	151 ± 8	258 ± 7	1,708 ± 142	–	88

[a] Hydrolysis of yeast RNA was measured by the increase in absorbance at 298.5 nm in 150 mM Tris, 2 mM EDTA, pH 7.5, at 25 °C. Hydrolysis of guanylyl(3′-5′)cytidine (GpC) was measured by the increase in absorbance at 280 nm in 100 mM MES, 100 mM NaCl, 2 mM EDTA, pH 6.0, at 25 °C. The specific activity for RNA hydrolysis was measured from initial absorbance changes in ΔOD/(min * mg) at 298.5 nm.

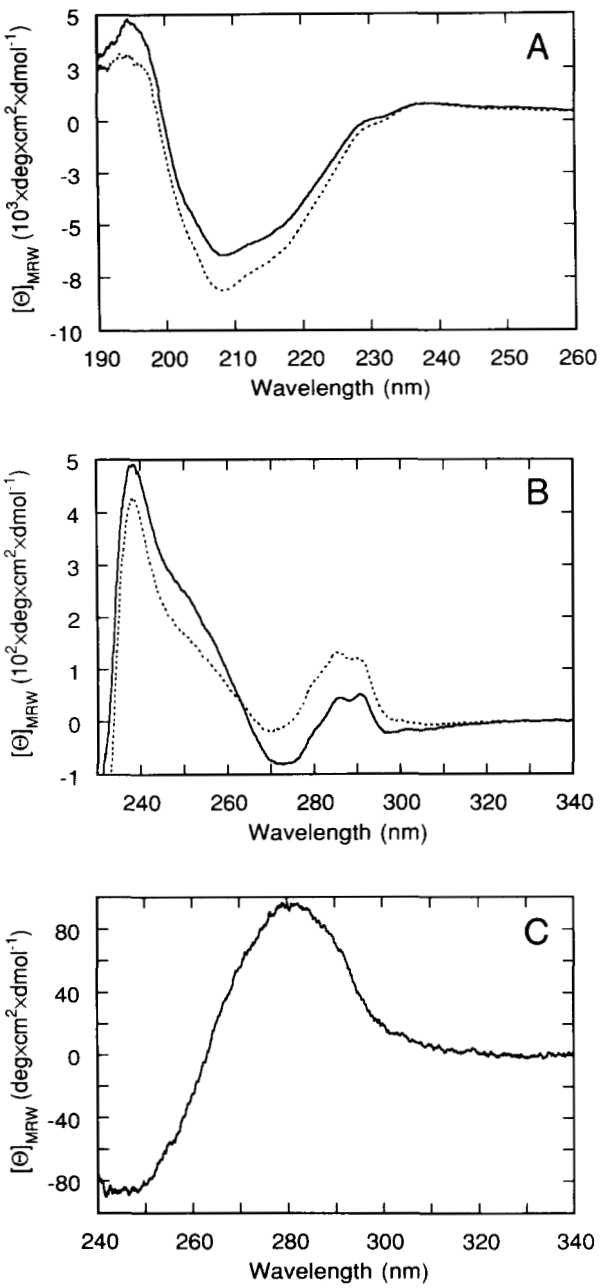

Fig. 2. CD spectra of wild-type RNase T1 (· · · · ·) and the C2S/C10N variant (———) in **(A)** the far-UV and **(B)** in the near-UV regions. The difference between both proteins in the near-UV (wild-type minus variant) is shown in **C**. The protein concentration was 180 μM in 0.01-cm cells for the far-UV CD and 22 μM in 1.0-cm cells for the near-UV CD. The solvent conditions were 0.1 M NaAc, pH 5.0, 25 °C.

shape to that of the wild-type protein, but is slightly shifted to more positive values throughout. In the region between 240 and 310 nm the fine structure of the aromatic bands around 280 nm is largely conserved, but the intensity of the CD is increased above 263 nm and decreased below 263 nm. The respective difference spectrum is shown in Figure 2C. Disulfide bonds are known to contribute to the CD in the near UV as well as in the far UV regions. The location of these bands depends strongly on the dihedral angle of the disulfides (Neubert & Carmack, 1974). With a dihedral angle of 78° (U. Heinemann, pers. comm.), the C2–C10 disulfide bond in wild-type RNase T1 should give rise to a positive band near 270 nm and a negative band near 235 nm in the near UV and to several bands in the far UV. Taken together, the maximum near 280 nm and the minimum near 245 nm in the difference spectrum (Fig. 2C) could reflect the contribution of the C2–C10 disulfide to the CD spectrum of native RNase T1. The overall similarity of the CD spectra in the far UV suggests that the secondary structure of the variant is largely conserved. The observed difference contains probably also contributions from the mutated disulfide. Changes in secondary structure, such as in the small 2-stranded β-sheet that is connected by the C2–C10 bridge, cannot be ruled out.

NMR spectra of C2S/C10N-RNase T1

The fingerprint regions (C_αH-NH crosspeaks) of the TOCSY spectra of C2S/C10N-RNase T1 and the wild-type protein are compared in Figure 3. Previous assignments for the wild-type protein were made at pH 5.5, 40 °C (Hoffmann & Rüterjans, 1988). Under these conditions the C2S/C10N variant is partially unfolded, and therefore the resonances of both proteins were assigned at pH 5.0, 25 °C, by a combination of Clean-TOCSY, DQF-COSY, and NOESY spectra in ^1H_2O and ^2H_2O. A detailed list of the assignments is found in Mayr (1993). A visual inspection of Figure 3A and 3B shows that most C_αH-NH crosspeaks are unaffected by the C2S/C10N substitution. The differences in the chemical shifts of the C_αH and the NH resonances between the C2S/C10N variant and the wild-type protein are plotted in Figure 4A and B as a function of the amino acid sequence. This comparison shows that the differences are largely confined to the amino-terminal chain region where the 2 mutations are located (see Kinemage 3). The chemical shifts (δ) of the C_αH and NH resonances depend on both the nature of the amino acid and on the electromagnetic environment of the peptide bond (Wüthrich, 1986; Wishart et al., 1991). The comparisons in Figure 4A and B therefore indicate that apart from local changes around the site of mutation, the backbone conformation of RNase T1 is not significantly altered by breaking the C2–C10 disulfide bond.

Further analysis of the NOESY spectrum of the C2S/C10N variant shows an extended region of d_{NN} connectivities for residues 13–29, corresponding to the single α-helix in the wild-type protein. This α-helix (cf. Fig. 1A) is apparently not affected by the removal of the C2–C10 disulfide bond. In addition, we determined by NMR spectroscopy the conformations of the peptide bonds preceding Pro 39 and Pro 55, which are *cis* in the wild-type protein (Hoffmann & Rüterjans, 1988; Martinez-Oyanedel et al., 1991). In the C2S/C10N variant, strong NOESY crosspeaks could be found both between C_αH(54) and C_αH(55), and between NH(54) and C_αH(55), which indicate a *cis* conformation of the Ser 54-Pro 55 peptide bond. In the variant, a strong NOESY crosspeak could also be detected for C_αH(38) and NH(40), which was used as evidence for a *cis* peptide bond at Tyr 38–Pro 39 in the wild-type protein (Hoffmann & Rüterjans, 1988). We therefore conclude that in spite of the strong destabilization of the protein by removing the C2–C10 disulfide bond (see below), the isomeric states of the peptide bonds preceding Pro 39 and Pro 55 are not changed.

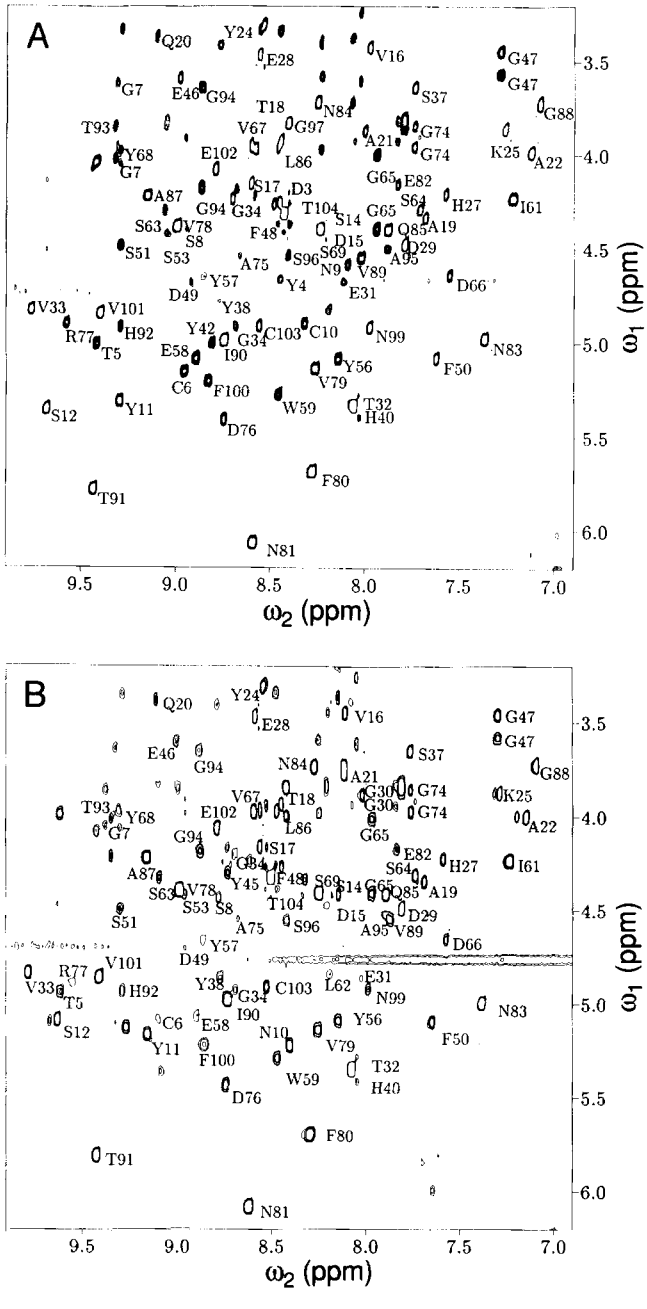

Fig. 3. Contour plot of the fingerprint regions (C_αH-NH) of the TOCSY spectra for **(A)** wild-type RNase T1 and **(B)** the C2S/C10N variant. The spectra were obtained at a protein concentration of 3 mM and solvent conditions of 0.02 M NaOx, pH 5.0, 25 °C. The parameters used for acquisition of the spectra are described in the Materials and methods section. The crosspeaks for the individual amino acids are labeled with the corresponding sequence position.

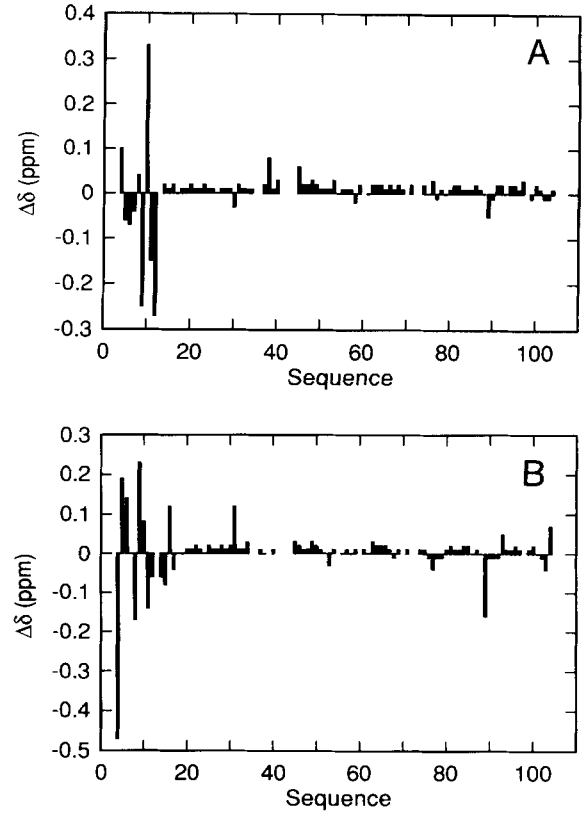

Fig. 4. Plots of the chemical shift difference versus amino acid sequence for wild-type RNase T1 minus the C2S/C10N variant for **(A)** the C_αH-protons and **(B)** the NH-protons. The assignments and the same conditions as in Figure 3 were used. In those cases where the assignment for either of the 2 proteins was missing, no difference value could be plotted.

GdmCl-induced unfolding transitions

Breaking of the C2–C10 disulfide bond markedly destabilizes RNase T1. GdmCl-induced unfolding transition curves of the C2S/C10N variant and the wild-type protein were measured at pH 5.0, 25 °C, by using different spectroscopic methods (Fig. 5A). Changes in secondary structure during unfolding were monitored by CD at 222 nm, changes in tertiary structure by absorbance at 287 nm and by fluorescence at 320 nm. After normalization, the 3 transition curves coincide (Fig. 5A), indicating that the C2S/C10N mutation did not change the 2-state character of the unfolding transition of RNase T1 (Kiefhaber et al., 1990d; Hu et al., 1992). The midpoint is decreased from 3.64 M (wild type) to 2.60 M (C2S/C10N variant). A linear dependence of the free energy of denaturation (ΔG_D) on GdmCl is observed, and similar slopes ($m = d\Delta G_D/d$[GdmCl]) are obtained for the wild-type protein and the C2S/C10N variant (Fig. 5B). Apparently, the cooperativity of unfolding was not affected by the C2S/C10N mutation. The m-value is a measure for the difference in interaction of the denaturant with the native and the denatured state (Tanford, 1968; Pace, 1986). The value of $\Delta G_D^{H_2O}$ obtained by linear extrapolation to 0 M GdmCl (Table 2) is reduced by 11.0 kJ/mol from 41.8 kJ/mol (wild-type protein) to 30.8 kJ/mol (C2S/C10N variant). Pace et al. (1988) reported for (2–10)-RCM-RNase T1 a slightly larger difference in $\Delta G_D^{H_2O}$ of 14.2 kJ/mol at pH 5.0, 12.5 °C. GdmCl-induced unfolding transitions of the C2S/C10N variant were measured also at 10 °C and at pH 8.0. The results, summarized in Table 2, indicate that an average m-value of 11.2 ± 1.0 kJ/(mol·M) is observed under all conditions for the mutated and for the wild-type protein. The estimates for the decrease in $\Delta G_D^{H_2O}$ ranged from 7.3 to 11.0 kJ/mol. The linear extrapolation procedure leads to

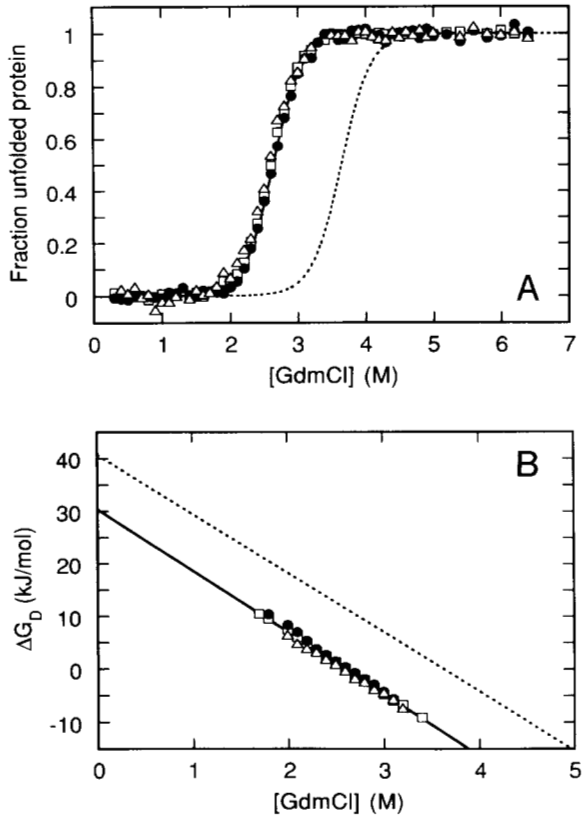

Fig. 5. Two-state analysis of the GdmCl-induced unfolding transitions. **A:** Fraction of unfolded protein. **B:** Linear extrapolation of the Gibbs free energy to determine the stability of the protein at 0 M GdmCl. The fraction of unfolded protein is derived from the experimental data by assuming a 2-state transition of unfolding. The values for the Gibbs free energy in the presence of GdmCl (ΔG_D) were calculated from the corresponding equilibrium constants (K_D) in the transition region. Circular dichroism at 222 nm (□), absorbance at 287 nm (△), and fluorescence at 320 nm (●) were used to monitor unfolding at a protein concentration of 9 μM. The solid line represents the curve fit of the data for the C2S/C10N variant; the dashed line represents the curve fit of the data for the wild-type protein. The solvent conditions were 0.1 M NaAc, pH 5.0, 25 °C. The midpoints are 2.60 M GdmCl for the C2S/C10N variant and 3.64 M GdmCl for the wild-type protein. Data for the wild-type protein are from Mayr et al. (1993b).

overestimates of $\Delta G_D^{H_2O}$ because RNase T1 is slightly stabilized by ion binding (Mayr & Schmid, 1993c). This should, however, cancel when differences in $\Delta G_D^{H_2O}$ are considered, as in the present case.

Thermal denaturation of C2S/C10N-RNaseT1

The destabilizing effect of the C2S/C10N mutation is also reflected in the thermal transition curves measured at different pH values. At pH 5.0, the midpoint of the transition (T_m) of the C2S/C10N variant is reduced by 7.1 °C relative to the wild-type protein (Fig. 6A), which agrees well with the decrease in T_m of 6.0 °C reported by Pace et al. (1988) for (2-10)-RCM-RNase T1 under similar conditions. Thermal unfolding transitions of the wild-type protein and the C2S/C10N variant were measured between pH 2 and pH 8. The pH profiles of the T_m values were very similar for wild-type RNase T1 and for the C2S/C10N variant, with maxima near pH 5 (Fig. 6B). The T_m values of the C2S/C10N variant are, however, decreased by 6.4–8.1 °C throughout the entire pH range.

The thermal unfolding transitions in Figure 6A can also be used to estimate the difference in Gibbs free energy of denaturation ($\Delta\Delta G_D^{H_2O}$) between the C2S/C10N variant and the wild-type protein. Since the change in heat capacity upon unfolding (ΔC_P) is not known for the C2S/C10N variant, the stabilities of the 2 forms of RNase T1 are compared at 56.5 °C, which is between the T_m values of the wild-type and the C2S/C10N proteins (cf. Fig. 6A). Thus, extrapolation can be avoided and a value of $\Delta\Delta G_D^{H_2O}$ of 9.7 kJ/mol is obtained. Taken together, these results indicate that the C2S/C10N variant of RNase T1 is about 10 kJ/mol less stable than the wild-type protein.

Unfolding and refolding kinetics

Unfolding and refolding of C2S/C10N-RNase T1 are reversible processes. Representative kinetics, as followed by the change in Trp fluorescence at 320 nm, are shown in Figure 7A and B. Unfolding induced by 6.0 M GdmCl (Fig. 7A) is a single first-order reaction, and its amplitude accounts for the entire change in fluorescence as expected from the equilibrium unfolding transition (cf. Fig. 5A). Unfolding of the C2S/C10N variant is about

Table 2. *Thermodynamic parameters for the GdmCl-induced unfolding transitions of wild-type RNase T1 and the C2S/C10N variant*[a]

	Wild type			C2S/C10N			
Conditions	$[GdmCl]_{1/2}$ (M)	$\Delta G_D^{H_2O}$ (kJ/mol)	*m*-value (kJ/mol * M)	$[GdmCl]_{1/2}$ (M)	$\Delta G_D^{H_2O}$ (kJ/mol)	*m*-value (kJ/mol * M)	$\Delta\Delta G_D^{H_2O}$ (kJ/mol)
pH 5, 10 °C	3.94	41.1	−10.4	3.24	33.8	−10.4	7.3
pH 5, 25 °C	3.64	41.8	−11.5	2.60	30.8	−11.6	11.0
pH 8, 10 °C	3.21	35.3	−11.0	2.28	27.8	−12.2	7.5
pH 8, 25 °C	2.40	24.7	−10.3	1.43	15.6	−10.9	9.1

[a] Unfolding transitions were measured by fluorescence at 320 nm (10-nm bandwidth) after excitation at 268 nm (1.5-nm bandwidth) in 1 × 1-cm cells. $\Delta G_D^{H_2O}$ and the *m*-values were derived from a 2-state analysis of the transitions by the method of Santoro and Bolen (1988). The protein concentration was 10 μM, and 0.1 M NaAc, pH 5.0, and 0.1 M Tris, pH 8.0, were used as buffers. Unfolding transitions at pH 5.0, 25 °C, were additionally measured by absorbance at 287 nm and by circular dichroism at 222 nm. They coincide with the fluorescence-detected transitions (Fig. 5).

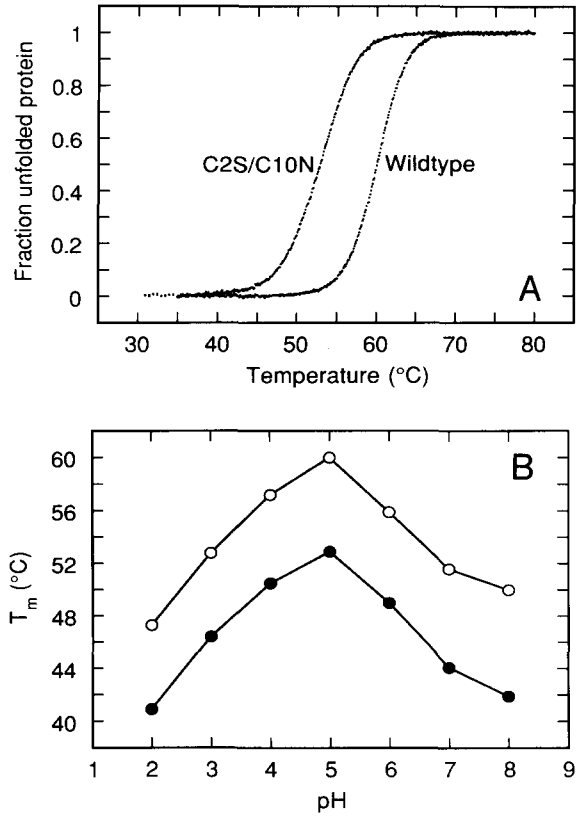

Fig. 6. A: Thermal unfolding transitions of C2S/C10N and wild-type RNase T1. The unfolding transitions in 0.1 M NaAc, pH 5.0, were monitored by the decrease in absorbance at 287 nm (2-nm bandwidth) at a rate of 0.3 °C/min (10 data points per degree). A linear extrapolation of the baselines in the pre- and posttransitional regions was used to determine the fraction of unfolded protein within the transition region by assuming a 2-state mechanism for unfolding. The protein concentration was 18 μM and the pathlength was 10 mm. The reversibility of unfolding was tested by subsequent cooling. **B:** pH-dependence of the midpoint of thermal denaturation, T_m, for wild-type RNase T1 (○) and the C2S/C10N variant (●). Thermal transitions as shown in Figure 6A at different pH values were used to determine T_m. The buffers used are listed in the Materials and methods.

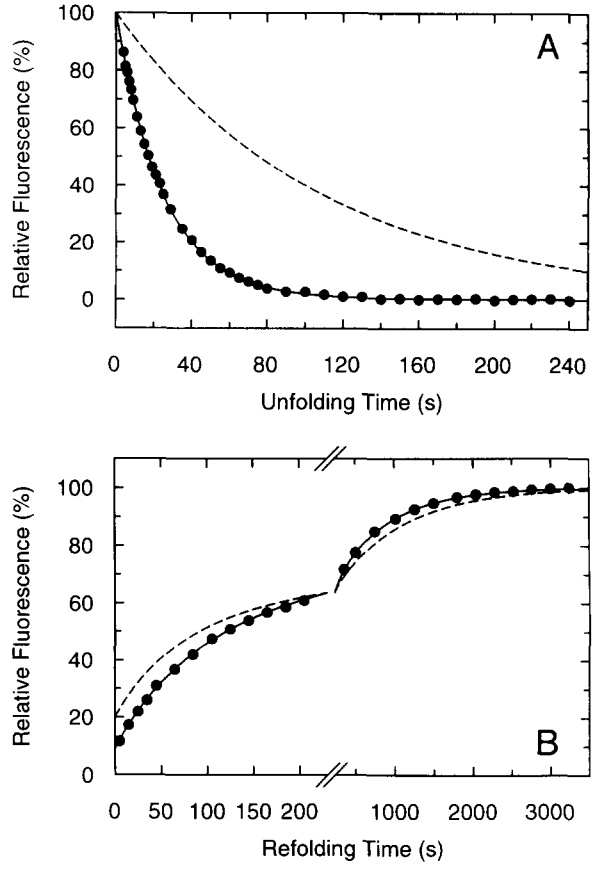

Fig. 7. Kinetics of **(A)** unfolding and **(B)** refolding of C2S/C10N-RNase T1 (●) and wild-type RNase T1 (---) at pH 5.0, 25 °C. The kinetics were monitored by fluorescence at 320 nm (10-nm bandwidth) after excitation at 268 nm (1.5-nm bandwidth) in 1 × 1-cm cells. The unfolding conditions were 6.0 M GdmCl, 0.1 M NaAc; the refolding conditions were 1 μM protein in 0.15 M GdmCl, 0.1 M NaAc. The fluorescence of the denatured and the native state was set as 0% and 100%, respectively, and the number of shown data points reduced for clarity. Unfolding of C2S/C10N-RNase T1 can be described by a single exponential (A = 100%, τ = 25.1 s), refolding by the sum of 2 exponentials (A_1 = 45%, τ_1 = 610 s; A_2 = 43%, τ_2 = 80 s), as indicated by the continuous lines.

4-fold faster than unfolding of the wild-type protein under the same conditions.

The refolding kinetics in 0.15 M GdmCl, pH 5.0, 25 °C, of the variant and the wild-type protein are very similar (Fig. 7B). In both cases slow refolding can be approximated by the sum of 2 exponential reactions. During the dead time of the experiment (less than 3 s) about 10% of the total amplitude in refolding is regained for the C2S/C10N variant and about 21% for the wild-type protein. This rapid reaction reflects the fast refolding of the U_F-species (about 2–4% of all molecules) and the formation of intermediates within several milliseconds (Kiefhaber et al., 1990b, 1990c, 1992c). The 2 slow phases in the folding of the C2S/C10N variant correspond closely to the "intermediate" and "very slow" phases in the folding of wild-type RNase T1. Both the rates and the amplitudes are similar for the 2 forms of RNase T1. These reactions are limited in rate by the isomerizations of the *cis* prolines 39 and 55 (Kiefhaber et al., 1990a, 1990b; Mayr & Schmid, 1993b; Mayr et al., 1993b).

Very similar kinetics are also obtained when the refolding of the C2S/C10N variant and the wild-type protein are probed by enzymatic activity (Fig. 8). In both cases 10–15% of the activity is regained in a rapid reaction. This early activity is due in part to the $U_F \rightarrow N$ reaction (about 2–4%) and in part to the rapid formation of partially active intermediates (Kiefhaber et al., 1990b). Further reactivation parallels the fluorescence detected refolding with similar amplitudes and rate constants (cf. Table 3).

A distinctive feature of the folding mechanism of wild-type RNase T1 is the formation of native molecules on 2 major folding routes (Kiefhaber et al., 1990a; Mayr et al., 1993a): a sequential reaction, in which the isomerization of Pro 39 is followed by the isomerization of Pro 55, and a very slow reaction, in which the order of the prolyl isomerizations is reversed. This reaction is very slow, because it involves the hindered *trans* to *cis* isomerization of Pro 39 in a largely folded intermediate (Kiefhaber et al., 1992a). This mechanism is not changed by the breaking of the C2–C10 disulfide bond in the 2CS/C10N vari-

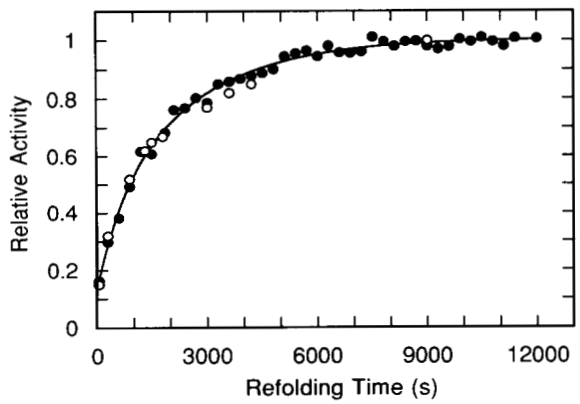

Fig. 8. Regain of enzymatic activity during refolding of C2S/C10N-RNase T1 (●) and wild-type RNase T1 (○) at pH 8.0, 10 °C. Enzymatic activity was measured by the cleavage of the dinucleotide GpC as described in the Materials and methods. The activity assay contained a 400-fold molar excess of trypsin to prevent further refolding of unfolded or partially folded molecules during the assay. The final activity was nearly identical in both cases and was set as 100%. Reactivation of C2S/C10N RNase T1 can be described by the sum of 2 exponentials (A_1 = 62%, τ_1 = 2,500 s; A_2 = 26%, τ_2 = 730 s) as shown by the continuous line.

ant. When the formation of native molecules during refolding is followed by unfolding assays (Fig. 9A) a time course is obtained for the folding of this variant that closely parallels the kinetics of the wild-type protein (taken from Kiefhaber et al., 1990a, 1990b). In both cases the data are well described by the folding mechanism of wild-type RNase T1. About 2% native molecules are formed in the fast refolding reaction within the dead time of this experiment (30 s; Fig. 9B), which agrees reasonably well with about 3.5% fast-folding species (U_F) observed for the wild-type protein (Kiefhaber et al., 1990a, 1990b).

The kinetics of refolding were measured under various conditions and by using different probes of structure formation. The results are summarized in Table 3. The time constants of

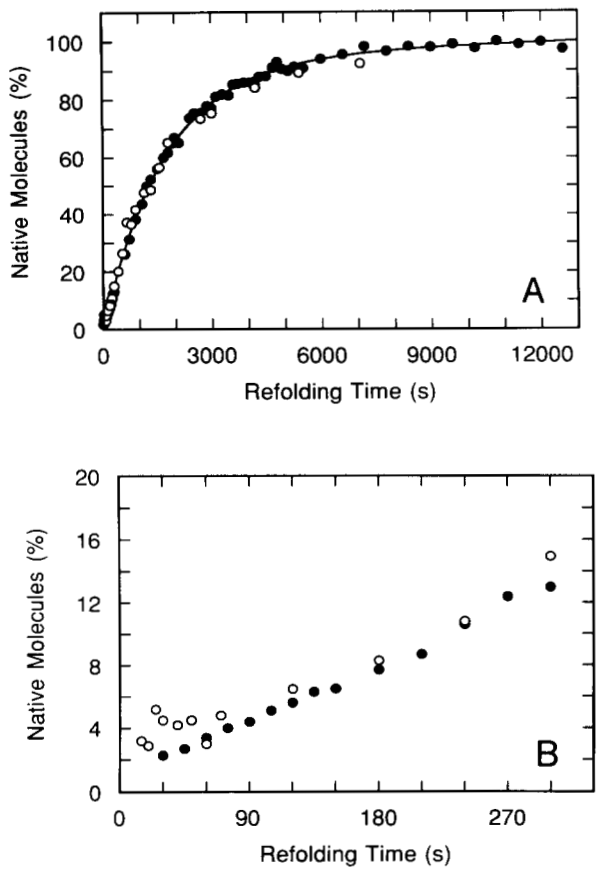

Fig. 9. Formation of native molecules during refolding of C2S/C10N RNase T1 (●) and wild-type RNase T1 (○) at pH 8.0, 10 °C. The percentage of native molecules present after various times of refolding was determined by the amplitudes of individual unfolding assays as described in the Materials and methods. The refolding conditions were 0.15 M GdmCl and 0.1 M Tris, pH 8.0; the unfolding conditions were 5.65 M GdmCl, 0.1 M Tris, pH 8.0. The protein concentration in the refolding step was 10 μM. The early time region of panel **A** is shown in panel **B**, to indicate the presence of about 2–4% fast-folding U_F species.

Table 3. *Refolding kinetics of wild-type RNase T1 and the C2S/C10N variant under various conditions*[a]

		Wild type				C2S/C10N			
Refolding conditions	Probe	τ_1 (s)	τ_2 (s)	A_1	A_2	τ_1 (s)	τ_2 (s)	A_1	A_2
pH 5.0, 25 °C	Fl	870	67	0.45	0.34	610	80	0.45	0.43
pH 5.0, 25 °C	Abs	820	67	0.34	0.33	600	78	0.47	0.39
pH 5.0, 10 °C	Fl	7,900	350	0.48	0.16	7,600	520	0.43	0.38
pH 5.0, 10 °C	Abs	8,400	350	0.38	0.13	6,800	560	0.42	0.39
pH 8.0, 25 °C	Fl	270	64	0.41	0.43	460		0.97	
pH 8.0, 25 °C	Abs	310	77	0.48	0.45	440		0.94	
pH 8.0, 10 °C	Fl	2,170	370	0.46	0.26	1,600	390	0.45	0.41
pH 8.0, 10 °C	Abs	3,000	450	0.36	0.22	1,860	440	0.47	0.34
pH 8.0, 10 °C	Act	2,500	300	0.68	0.22	2,500	730	0.62	0.26

[a] The refolding conditions were 0.15 M GdmCl and 0.1 M NaAc, pH 5.0, or 0.1 M Tris, pH 8.0. The protein concentrations for refolding were 1 μM for fluorescence (Fl), 7 μM for absorbance (Abs), and 0.15 μM for the regain of enzymatic activity (Act). The amplitudes (A_1, A_2) are given as fractions of the total difference between the native and the denatured protein as expected from the corresponding equilibrium unfolding transitions. For C2S/C10N RNase T1, phases 1 and 2 merge at pH 8.0, 25 °C, and single values for τ and A are given.

both the very slow (τ_1) and the intermediate phase (τ_2) were found to be very similar for the C2S/C10N variant and the wild-type protein under conditions where the folded state shows a high conformational stability (at pH 5.0 and at pH 8.0, 10 °C). Consistently, however, the very slow reaction was slightly faster in the folding of the variant protein. This reaction is limited in rate by the *trans* to *cis* isomerization of Pro 39. The amplitudes of the slow folding reactions are generally larger for the C2S/C10N variant than for the wild-type protein. This indicates that the signal changes in the dead time are smaller, presumably because the rapidly formed intermediates are less well ordered or less stable when the protein is destabilized by breaking the C2–C10 disulfide bond. At pH 8.0 and 25 °C, the 2 slow refolding phases of the variant protein merge, since the transition region is approached already under these conditions. A similar merging of the slow phases is observed for the wild-type protein as well, albeit at higher concentrations of GdmCl.

Dependence on GdmCl concentration of the folding kinetics

The unfolding and refolding kinetics of C2S/C10N-RNase T1 were measured as a function of the concentration of GdmCl (Fig. 10) and compared with the folding kinetics of the wild-type protein (Kiefhaber & Schmid, 1992). Figure 10A shows the initial and the final fluorescence values observed in the individual kinetic experiments. The final values closely follow the equilibrium unfolding transition (cf. Fig. 5A), indicating that, as for the wild-type protein, the unfolding and refolding reactions of C2S/C10N-RNase T1 are reversible in the entire range of GdmCl concentrations. At low residual concentrations of GdmCl (0.15–1.0 M GdmCl), the total change in fluorescence intensity during slow refolding is less than expected, indicating that intermediates are formed rapidly within the dead time of 3 s (Kiefhaber et al., 1990b, 1990c). The stability of these intermediates is apparently lower in the case of the C2S/C10N variant, because such a "missing amplitude" is observed only below 1 M GdmCl (Fig. 10A). In the folding of the wild-type protein it persists up to about 2 M GdmCl (Kiefhaber & Schmid, 1992).

The time constants of unfolding and refolding of C2S/C10N-RNase T1 are shown as a function of the GdmCl concentration in Figure 10B together with the respective data for the wild-type protein (taken from Kiefhaber & Schmid, 1992). The refolding kinetics of the C2S/C10N variant are biphasic from 0 M to 1.5 M GdmCl. In this concentration range the relative amplitude of the faster phase decreases continuously in favor of the relative amplitude of the very slow phase and reaches zero near 1.5 M GdmCl (Fig. 10C). Above 1.5 M GdmCl, refolding as well as unfolding are virtually single first-order reactions, which account for the entire change in fluorescence (Fig. 10A). This is expected from theoretical models for folding in the absence of partially folded intermediates (Kiefhaber et al., 1992b).

The comparison of the GdmCl profiles for the very slow phases of both variants of RNase T1 reveals some interesting similarities but also differences. The time constants of refolding are virtually identical in the presence of 0.15 M GdmCl (cf. also Table 3). This similarity does, however, not extend to higher concentrations of denaturant. Between 0.15 M and 1.0 M GdmCl, refolding of the wild-type protein becomes slightly slower, but the refolding of the C2S/C10N variant becomes faster. These trends are then inverted, until identical kinetics are again observed near 1.5 M GdmCl. From 1.5 M to 3 M GdmCl, folding of the wild-type protein is faster than folding of the variant. These seemingly complex differences can readily be explained by assuming that the entire profile for the very slow

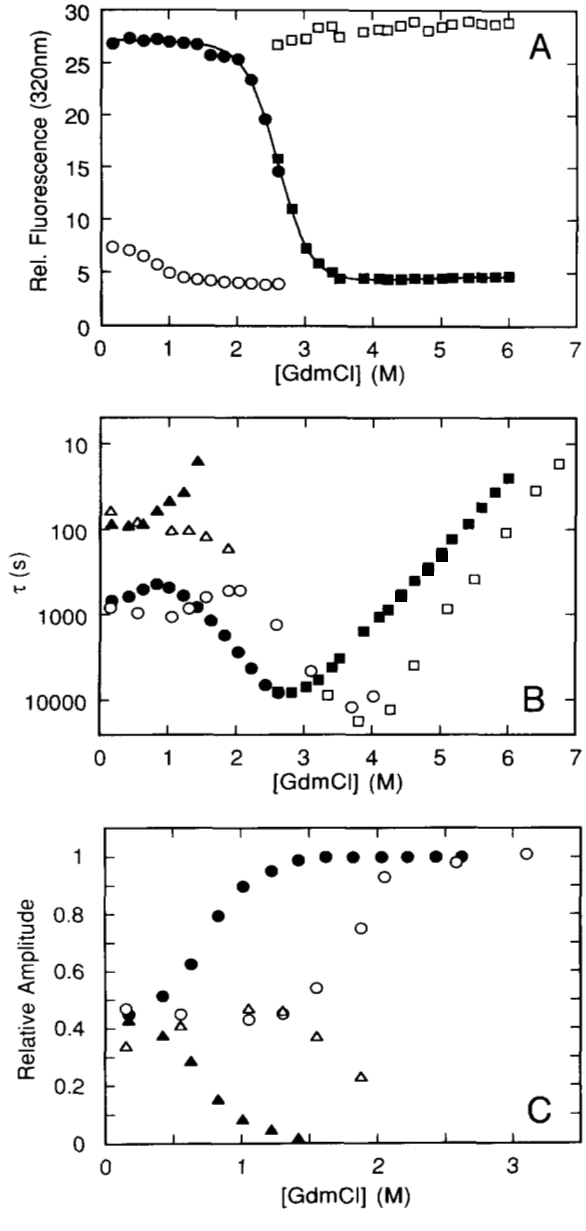

Fig. 10. Dependence on GdmCl concentration of the folding kinetics. **A:** GdmCl-induced unfolding transition of C2S/C10N RNase T1. The fluorescence values observed at t_∞ of the refolding (●) and unfolding (■) reactions were used to determine the folding transition. Additionally, the initial values for the slow refolding (○) and unfolding (□) kinetics are shown. **B:** GdmCl-dependent refolding and unfolding kinetics of C2S/C10N RNase T1 (●, ■, ▲) and wild-type RNase T1 (○, □, △). Slow refolding is biphasic below 1.0 M GdmCl for the C2S/C10N variant and below 2.0 M for the wild-type protein, as indicated by (●, ▲) and (○, △). Unfolding is monophasic for both proteins, as indicated by (■, □). **C:** Refolding amplitudes of C2S/C10N RNase T1 and wild-type RNase T1 for the slower (●, ○) and the faster phases (▲, △) in refolding. The kinetics of unfolding and refolding were measured in 0.1 M NaAc, pH 5.0, 25 °C, by the change in fluorescence at 320 nm. Data for the wild-type protein are taken from Kiefhaber and Schmid (1992).

folding reaction of the variant is shifted by approximately 1.0 M to lower GdmCl concentrations. A shift by 1 M GdmCl would lead to an almost perfect superposition of the 2 profiles in Figure 10B and also for the corresponding amplitudes in Figure 10C. Possible molecular explanations for this shift will be considered in the Discussion. An interpretation of the differences in the time constants of the faster phases is not warranted, because their amplitudes decrease strongly with increasing concentration of GdmCl.

Efficiency of prolyl isomerase (PPI)

All slow steps in the refolding of wild-type RNase T1 with intact disulfides involve isomerizations of prolyl peptide bonds and are accelerated by PPI (Fischer et al., 1989). The individual slow reactions are catalyzed with different efficiencies (Schönbrunner et al., 1991). The processes that constitute the intermediate phase are well catalyzed, whereas *trans* to *cis* isomerization of Pro 39 in the very slow reaction is only marginally accelerated.

The slow refolding reactions of the C2S/C10N variant are also catalyzed by PPI, as shown by the comparison of the kinetics in the absence and in the presence of 1,000 PU/mL PPI (Fig. 11). In the presence of PPI the intermediate phase of refolding can be resolved into 2 processes that differ in the extent of catalysis (Fig. 12A). This was observed previously for the wild-type protein as well (Schönbrunner et al., 1991). The rates of these 2 folding reactions depend in identical manner on PPI concentration for C2S/C10N-RNase T1 and the wild-type protein (Fig. 12A). A different behavior was, however, found for the *trans* to *cis* isomerization of Pro 39 in the very slow phase. This major folding reaction is not well catalyzed in the folding of the wild-type protein, because rapid formation of ordered structure in a folding intermediate renders this bond almost inaccessible for PPI. When the C2–C10 disulfide bond is broken, this refolding reaction is much better catalyzed by PPI (Fig. 12B).

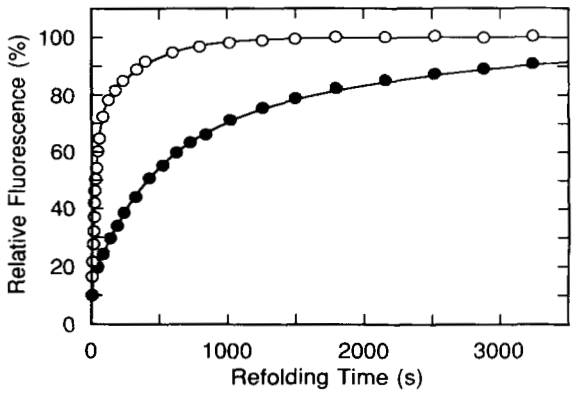

Fig. 11. Refolding of C2S/C10N RNase T1 in the absence and in the presence of prolyl isomerase at pH 8.0, 10 °C. Refolding was monitored after excitation at 268 nm (1.5-nm bandwidth) by fluorescence at 320 nm (10-nm bandwidth) in 1 × 1-cm cells. The refolding conditions were 1 μM protein in 0.15 M GdmCl, 0.1 M Tris, pH 8.0, 10 °C. The fluorescence of the denatured and the native states was set as 0% and 100%, respectively. A kinetic analysis of the data as the sum exponentials resulted in $A_1 = 45\%$, $\tau_1 = 1{,}603$ s; $A_2 = 41\%$, $\tau_2 = 389$ s; $A_3 = 9\%$, $\tau_3 = 9.1$ s in the absence of PPI (●), and in $A_1 = 33\%$, $\tau_1 = 200$ s; $A_2 = 61\%$, $\tau_2 = 16$ s in the presence of 1,000 PU/mL PPI (○).

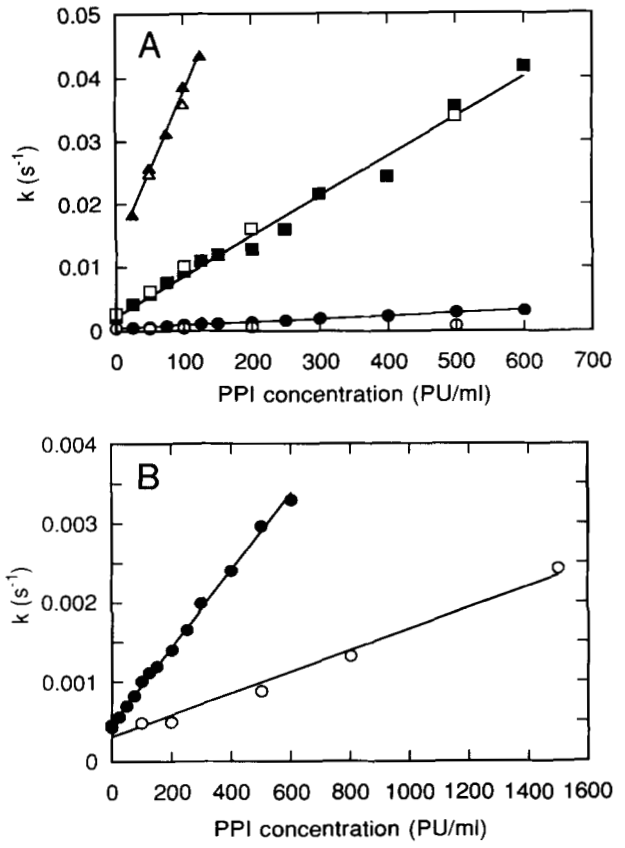

Fig. 12. Rate constants of the slow steps in folding of wild-type and of C2S/C10N RNase T1 as a function of the concentration of PPI. **A:** Effect of PPI on the rate constants of slow folding. Refolding at 10 °C was measured in 0.15 M GdmCl and 0.1 M Tris, pH 8.0, 10 °C, as in Figure 11 by the increase in fluorescence at 320 nm. Experimental data for refolding were analyzed as the sum of 3 exponentials. The very slow phases of refolding are represented by circles (○, ●), the medium phases by squares (□, ■), and the faster phases by triangles (△, ▲). Open symbols refer to the wild-type and closed symbols to the C2S/C10N protein, respectively. **B:** Replot of the data for the slowest phase to document the difference in catalysis by PPI.

This is probably not a direct effect of the mutation. Rather, it is mediated by the general destabilization caused by the C2S/C10N mutation, which, in turn, also destabilizes partially folded intermediates.

Discussion

The folded structure of RNase T1 is largely maintained after the breaking of the C2–C10 disulfide bond in the C2S/C10N variant. As judged by CD and by 2D-NMR, the backbone conformation is almost unaffected, and significant differences between the wild type and the C2S/C10N variant were found only in the amino-terminal chain region, where the cysteine residues 2 and 10 are located. Nativelike conformations were also found for variants of bovine pancreatic trypsin inhibitor and of lysozyme that lacked single disulfide bonds (Stassinopoulou et al., 1984; States et al., 1987; Eigenbrot et al., 1990; van Mierlo et al., 1991). A functional active site is indicated by the high catalytic activity of the C2S/C10N variant. A similarly high activity was also found for the single disulfide variant (2–10)-RCM-RNase

T1, which was produced by selective reduction and carboxymethylation of the C2–C10 bond (Pace et al., 1988).

In contrast to these minor changes in structure, the C2S/C10N mutation has a moderate destabilizing effect on RNase T1, and the Gibbs free energy of denaturation is decreased by about 11 kJ/mol. Pace et al. (1988) modified previous formalisms (Schellman, 1955; Poland & Scheraga, 1965) and proposed an equation to calculate the decrease in entropy caused by covalent crosslinks in unfolded protein chains. By using their formula (Equation 4 in Pace et al., 1988) we would expect a loss in Gibbs free energy of 10.3 kJ/mol after opening the C2–C10 crosslink at 25 °C, in fair agreement with the experimental values (cf. Table 2). This good coincidence should, however, be regarded as fortuitous, since the effects on the folded state of breaking the covalent crosslink and of replacing cysteine residues 2 and 10 by a serine and an asparagine, respectively, are not accounted for in the above treatment. Tidor and Karplus (1993) suggested that the breaking of a disulfide should stabilize proteins by increasing the entropy of the folded state, in particular when the disulfide is exposed as the C2–C10 bond of RNase T1, because a disulfide bond immobilizes potentially flexible regions of the protein.

Breaking of the C2–C10 disulfide does not change the folding mechanism of RNase T1. The folding reactions of the C2S/C10N variant are well explained by the kinetic model of the wild-type protein, with slow reactions that are limited in rate by the *trans* to *cis* isomerizations of Pro 39 and Pro 55. Small changes were observed for the very slow *trans* to *cis* isomerization of Pro 39. Pro 39 is inaccessible to solvent in native RNase T1 and presumably also in a folding intermediate that is formed rapidly under strongly native conditions and retards Pro 39 isomerization. When the C2–C10 bond is broken, *trans* to *cis* isomerization of Pro 39 is slightly accelerated and 4 times better catalyzed by prolyl isomerase. We do not think that the breaking of the C2–C10 disulfide bond has a direct long-range effect on the isomerization of Pro 39 and its catalysis during folding. Rather, the disruption of this crosslink leads to a general destabilization of folding intermediates in a similar manner as it destabilizes the native protein. Thus, the stability of the early intermediates is decreased, the structural barrier to isomerization of Pro 39 is slightly reduced, and the accessibility of the Tyr 38–Pro 39 bond for prolyl isomerase is improved. The differences in the GdmCl profiles of the slow refolding reactions in Figure 10 are also well explained by the destabilizing effect of the C2S/C10N mutation. The profiles for the time constants and the amplitudes are almost indistinguishable, when they are compared at equal distance from the respective transition midpoint, which is at 3.64 M GdmCl for the wild-type protein and at 2.60 M GdmCl for the C2S/C10N variant. In other words, identical kinetics are observed, when folding is compared under conditions of equal stability of the folded proteins and, presumably, equal stability of partially folded intermediates. Apparently, breaking of the C2–C10 bond has the same effect on the stability and on the folding kinetics of RNase T1 as adding 1 M GdmCl to the wild-type protein.

In earlier work in this field, additional crosslinks were introduced into lysozyme and RNase A by chemical modification and the stability and the folding kinetics of these derivatives were determined. In both cases the stabilities of the proteins were increased by the extra crosslinks. An increase in the rate of refolding was observed for lysozyme, but a decrease in the rate of unfolding for RNase A (Lin et al., 1984, 1985; Segawa & Sugihara, 1984; Segawa & Kume, 1986). It should be noted in these comparisons that prolyl isomerizations are involved in the folding of RNase A and RNase T1, but not of lysozyme.

In several models, folding is viewed as an ordered process in which tertiary structure formation is preceded by the formation of secondary structure (Kim & Baldwin, 1990; Matthews, 1993), or where the high resolving power of the tertiary interactions selects and stabilizes ordered local structure (Gō, 1983). The temporal order and correct interrelationship between these folding events is a central aspect in all these attempts to model the folding pathway. Our results indicate that for the folding of RNase T1 it is unimportant whether the interaction between cysteine residues 2 and 10 is covalently fixed throughout folding or not present at all.

In summary, breaking the C2–C10 disulfide bond has only a minor effect on the structure of RNase T1, but leads to a major loss of stability. The folding kinetics reflect this destabilization: folding of the wild-type protein and the C2S/C10N variant becomes identical when compared under conditions of equal stability. We conclude that the presence of a stable tertiary contact between Cys 2 and Cys 10 throughout the folding process does not change the mechanism of slow refolding.

Materials and methods

Materials

Enzymes for cloning were from Gibco BRL (Berlin, Germany), nucleotides and enzyme substrates from Sigma (St. Louis, Missouri). Oligonucleotides were purchased from TIB Molbiol (Berlin, Germany), GdmCl (ultrapure) from Schwarz/Mann (Orangeburg, New York), yeast RNA from Boehringer Mannheim (Mannheim, Germany), and guanylyl(3′-5′)cytidine from Pharma Waldhof (Düsseldorf, Germany). All other chemicals (analytical grade) were from Merck (Darmstadt, Germany). Recombinant human prolyl isomerase (cyclophilin A) was a kind gift of Sandoz AG (Basel, Switzerland). PPI activities are given as peptide acceleration units per milliliter (PU/mL), as defined by Mücke and Schmid (1992). The PPI used had an activity of approximately 8×10^5 PU/μmol.

Site-directed mutagenesis and protein purification

Mutagenesis of an *Escherichia coli* strain DH5α harboring the plasmid pA2T1 with the corresponding gene for RNase T1 was done by using the polymerase chain reaction as described previously (Landt et al., 1990). The mutagenesis primer was 5′-A GTT GTT AGA ACC GCA AGT GTA GTC CGA TGC-3′ (base substitutions for Ser 2 and Asn 10 are underlined). Wild-type RNase T1 and the C2S/C10N variant were both purified as described (Mayr & Schmid, 1993a). The amino acid substitutions in purified C2S/C10N-RNase T1 were confirmed by sequencing of the first 12 N-terminal amino acids.

Spectroscopic characterization

Concentrations of wild-type RNase T1 and the C2S/C10N variant were determined spectrophotometrically by using an absorption of 1.9 at 278 nm for a 1-mg/mL solution (Takahashi et al., 1970). For optical measurements, a Jasco J600 spectropolarim-

eter, a Kontron Uvikon 860 spectrophotometer, and a Hitachi F-4010 fluorimeter with integrated magnetic stirrers were used. All spectrometers had thermostatable cell holders or thermostatable cells.

CD spectra were measured at protein concentrations of 180 μM in 0.1-mm cells (far-UV CD) and of 22 μM in 10-mm cells (near-UV CD). The bandwidth was 1 nm, and spectra were accumulated 12 times in the far-UV region and 16 times in the near-UV region.

Steady-state kinetics

The activity assays were performed with a Shimadzu 160A spectrophotometer in 10-mm or 2-mm cells thermostated at 25 °C. To measure RNA hydrolysis (Oshima et al., 1976), a solution of yeast RNA (4.1 mg/mL in 150 mM Tris, pH 7.5, 2 mM EDTA) was preincubated in the spectrophotometer cell for 2 min to check for the absence of autolysis. Then 2–10 μL of enzyme solution were added to start the reaction. The final concentration of RNase was between 50 nM and 4 μM. The hydrolysis reaction was monitored by the increase in absorbance at 298.5 nm for 3–10 min, and the initial slope ($\Delta A_{298.5}$/[min·mg]) was determined. The cleavage of GpC was followed by the increase in absorbance at 280 nm. The concentration of GpC was determined by using an absorption coefficient of 12,600 M^{-1} cm^{-1} at 280 nm, and the amount of cleaved GpC was calculated by using a difference absorption coefficient of 2,200 M^{-1} cm^{-1} (Zabinski & Walz, 1976). The assay was carried out as follows: The GpC substrate was dissolved at different concentrations from 5 to 500 mM in 100 mM MES, pH 6.0, 100 mM NaCl, 2 mM EDTA. The reaction was started by adding 1 μL enzyme solution to give a final concentration of 3 nM. Initial velocities were determined as triplicates for at least 13 different substrate concentrations, recording the absorbance increase as ΔOD/min at 280 nm. The kinetic parameters were calculated with the help of the program Enzfitter (BIOSOFT Software, Cambridge, UK).

NMR spectroscopy

All 2D ^{1}H-NMR spectra were obtained on a Bruker AMX-600 spectrometer at 25 °C with spectral widths of 7,215 Hz in both dimensions. The software package N-dee (BIOSTRUCTURE Software, Strasbourg, France) was used to transform and analyze the spectra.

The samples for 2D ^{1}H-NMR spectroscopy were prepared in the following way: Desalted and lyophilized protein was dissolved in 1 mL 10 mM NaOx, adjusted to pH 5.0, and then lyophilized again. For experiments in ^1H_2O solution, samples were then dissolved in 500 μL of $^1H_2O/^2H_2O$ (9:1, v/v) at a protein concentration of 3 mM. For experiments in ^2H_2O solution, the samples were dissolved for 24 h in ^2H_2O (99.98%) at 25 °C, lyophilized, and again dissolved in ^2H_2O (99.996%) at a protein concentration of 3 mM.

The DQF-COSY spectra (Marion & Wüthrich, 1983; Rance et al., 1983) were collected as 4,096 × 700 data points. Clean-TOCSY spectra (Braunschweiler & Ernst, 1983; Griesinger et al., 1988) with 65-ms mixing periods were accomplished using an MLEV-17 pulse (Bax & Davies, 1985) and 4,096 × 512 data points. NOESY spectra (Kumar et al., 1980; Macura & Ernst, 1980) were collected with 150–250-ms mixing times as 4,096 × 512 data points. The COSY spectra were processed in both dimensions by a $\pi/12$ shifted sine bell, NOESY and TOCSY spectra by a $\pi/6$ shifted squared sine bell. After zero-filling to 4,096 × 2,048 data points, the digital resolution was 1.76 Hz/point in the ω_2-direction and 3.52 Hz/point in ω_1-direction. A baseline correction was performed for all spectra using a 5th-order polynomial. The chemical shift was calibrated using DSS (4,4-dimethyl-4-silapentane-5-sulfonate) as a reference.

GdmCl-induced denaturation

Native protein was incubated in 0.1 M NaAc, pH 5.0, in the presence of various concentrations of GdmCl until the folding/unfolding equilibrium was attained (12–48 h, depending on temperature). The extent of unfolding was determined for each solution by measuring the fluorescence at 320 nm (after excitation at 268 nm), absorbance at 287 nm, and CD at 222 nm. Absorbance and fluorescence were measured in 10-mm cells with thermostatable cell holders; CD was measured in thermostatable 5-mm cells. The protein concentration was 9 μM. A nonlinear least-squares fit of the experimental data by the method of Santoro and Bolen (1988) was used to obtain the *m*-values and $\Delta G_D^{H_2O}$ for each unfolding transition. The GdmCl concentrations of the samples were determined by measuring their refractive index (Pace, 1986).

Thermal denaturation and stability curves

Thermal denaturation curves were followed by the decrease in absorbance at 287 nm in a Gilford response II spectrophotometer equipped with a 6-position thermostatable cuvette holder and an integrated temperature programmer at a protein concentration of 18 μM. A resolution of 10 data points per degree, a heating rate of 0.3 °C/min, and a pathlength of 10 mm were used. Unfolding was reversible to ≥98% as judged by the coincidence of heating and subsequent cooling transitions in experiments where unfolding was arrested 12 °C above the T_m values for about 10 min. Prolonged incubation of the C2S/C10N variant at higher temperature caused slow irreversible aggregation. The values of T_m (midpoint of thermal transition) were obtained as described previously (Mayr et al., 1993b) by a nonlinear least-squares fit of the experimental data. To determine the pH dependence of the stability, the following buffers were used at a concentration of 0.1 M: glycine/HCl, pH 2 and 3; NaAc, pH 4 and 5; sodium cacodylate/HCl, pH 6 and 7; PIPES, pH 8.0.

Unfolding and refolding kinetics

Unfolding and refolding of C2S/C10N-RNase T1 was initiated by a 40-fold dilution of the protein (in 0.01 M NaAc, pH 5.0, or in 6.0 M GdmCl, 0.01 M NaAc, pH 5.0) with solutions of varying concentrations of GdmCl to give 0.15–6.0 M GdmCl in 0.1 M NaAc, pH 5.0. Experiments at pH 8.0 were carried out in the presence of 0.1 M Tris buffer. Complete mixing was achieved within about 3 s by rapid stirring. The kinetics of unfolding or refolding were followed by the changes in fluorescence at 320 nm (10-nm bandwidth) after excitation at 268 nm (1.5-nm bandwidth) or by the changes in absorbance at 287 nm (2-nm bandwidth). Final protein concentrations were 1 μM in fluorescence and 7 μM in absorbance. The kinetics were analyzed as the sum of exponential reactions by using the programs Kinfit (OLIS

Software, Bogart, Georgia) and Grafit (ERITHACUS Software, Staines, UK). The kinetic amplitudes were given as fractions of the signal changes observed in the corresponding equilibrium unfolding transitions under the same conditions. The concentrations of GdmCl were determined after the experiments by measuring the refractive index (Pace, 1986).

Reactivation measurements

Denatured protein in 6.0 M GdmCl, 0.01 M NaAc, pH 5.0, was diluted 40-fold to give refolding conditions of 0.15 μM C2S/C10N-RNase T1 in 0.15 M GdmCl, 0.1 M Tris, pH 8.0, 10 °C. After various times (t_i) of refolding, aliquots were drawn and diluted 30-fold into a GpC solution (in 10 mM Tris, 2 mM EDTA, pH 7.5) at 10 °C. The GpC solution contained a 400-fold molar excess of trypsin to prevent further folding of unfolded or partially folded protein molecules during the assay. Native C2S/C10N-RNase T1 and the wild-type protein are insensitive to trypsin under these conditions (Mayr & Schmid, unpubl. data). The concentration of GpC in the assay was 40 μM. The increase in absorbance at 257 nm caused by the cleavage of GpC by C2S/C10N-RNase T1 was recorded for 5 min. The value of ΔA_{257}/min was used as a measure of the enzymatic activity present after various times of refolding (t_i). The activity observed after complete refolding was set as 1.0.

Formation of native molecules during refolding

The formation of native molecules was determined by unfolding assays as described in detail by Mayr and Schmid (1993b). Denatured C2S/C10N-RNase T1 (450 μM) in 4.5 M GdmCl, 0.01 M NaAc, pH 5.0, was diluted 30-fold with 0.1 M Tris, pH 8.0, 10 °C, to initiate refolding. After various times (t_i) of refolding, samples were withdrawn and diluted 15-fold into a fluorimeter cell to give final unfolding conditions of 5.65 M GdmCl, 0.1 M Tris, pH 8.0, at 10 °C. The resulting unfolding kinetics were measured by the decrease in fluorescence at 320 nm after excitation at 268 nm. The amplitudes of the unfolding reactions (A_i) are a measure of the number of native molecules present after various times (t_i) of refolding. Part of the protein was allowed to refold completely. The respective unfolding assay (at $t = t_\infty$) yields the maximal amplitude (A_∞), which is proportional to the maximal number of native molecules that could be formed. The ratio of A_i/A_∞ gives the fraction of native molecules formed after t_i. Folding intermediates do not interfere, because under the assay conditions they unfold within the dead time of manual mixing. The protein concentration was 15 μM in the refolding step and 1 μM in the unfolding assay. A least-squares fit of the data from unfolding assays to the kinetic model for slow steps in refolding of RNase T1 was carried out by using the program Kaleidagraph (SYNERGY Software, Reading, PA, USA).

Acknowledgments

We thank C. Frech, U. Hahn, M. Mücke, and S. Walter for stimulating discussions. Advice on the NMR experiments and the software package N-dee from P. Bayer, A. Eijchart, F. Herrmann, R. Hofmann, and P. Rösch is deeply acknowledged. This work was supported by grants from the Deutsche Forschungsgemeinschaft (to F.X.S.) and from the Fonds der Chemischen Industrie (to L.M.M. and F.X.S.).

References

Baldwin RL. 1993. Pulsed H/D-exchange studies of folding intermediates. *Curr Opin Struct Biol 3*:84-91.

Bax A, Davies DG. 1985. MLEV-17-based two-dimensional homonuclear magnetization transfer spectroscopy. *J Magn Reson 65*:355-360.

Braunschweiler L, Ernst RR. 1983. Coherence transfer by isotropic mixing: Application to proton correlation spectroscopy. *J Magn Reson 53*: 521-528.

Eigenbrot C, Randal M, Kossiakoff AA. 1990. Structural effects induced by removal of a disulfide-bridge: The X-ray structure of the C30A/C51A mutant of basic pancreatic trypsin inhibitor at 1.6 Å. *Protein Eng 3*:591-598.

Fischer G, Wittmann LB, Lang K, Kiefhaber T, Schmid FX. 1989. Cyclophilin and peptidyl-prolyl *cis-trans* isomerase are probably identical proteins. *Nature 337*:476-478.

Gō N. 1983. Theoretical studies of protein folding. *Annu Rev Biophys Bioeng 12*:183-210.

Griesinger C, Otting G, Wüthrich K, Ernst RR. 1988. Clean TOCSY for ^{1}H spin system identification in macromolecules. *J Am Chem Soc 110*: 7870-7872.

Heinemann U, Saenger W. 1982. Specific protein-nucleic acid recognition in ribonuclease T1-2′-guanylic acid complex: An X-ray structure. *Nature 299*:27-31.

Hoffmann E, Rüterjans H. 1988. Two-dimensional ^{1}H-NMR investigation of ribonuclease T1. *Eur J Biochem 177*:539-560.

Hu CQ, Sturtevant JM, Thomson JA, Erickson RE, Pace CN. 1992. Thermodynamics of ribonuclease T1 denaturation. *Biochemistry 31*:4876-4882.

Jaenicke R. 1991. Protein folding: Local structures, domains, subunits, and assemblies. *Biochemistry 30*:3147-3161.

Kiefhaber T, Grunert HP, Hahn U, Schmid FX. 1990a. Replacement of a *cis* proline simplifies the mechanism of ribonuclease T1 folding. *Biochemistry 29*:6475-6480.

Kiefhaber T, Grunert HP, Hahn U, Schmid FX. 1992a. Folding of RNase T1 is decelerated by a specific tertiary contact in folding intermediates. *Proteins Struct Funct Genet 12*:171-179.

Kiefhaber T, Kohler HH, Schmid FX. 1992b. Kinetic coupling between protein folding and prolyl isomerization. I. Theoretical models. *J Mol Biol 224*:217-229.

Kiefhaber T, Quaas R, Hahn U, Schmid FX. 1990b. Folding of ribonuclease T1. 1. Existence of multiple unfolded states created by proline isomerization. *Biochemistry 29*:3053-3060.

Kiefhaber T, Quaas R, Hahn U, Schmid FX. 1990c. Folding of ribonuclease T1. 2. Kinetic models for the folding and unfolding reactions. *Biochemistry 29*:3061-3070.

Kiefhaber T, Schmid FX. 1992. Kinetic coupling between protein folding and prolyl isomerization. II. Folding of ribonuclease A and ribonuclease T1. *J Mol Biol 224*:231-240.

Kiefhaber T, Schmid FX, Renner M, Hinz HJ, Hahn U, Quaas R. 1990d. Stability of recombinant Lys 25-ribonuclease T1. *Biochemistry 29*:8250-8257.

Kiefhaber T, Schmid FX, Willaert K, Engelborghs Y, Chaffotte A. 1992c. Structure of a rapidly formed intermediate in RNase T1 folding. *Protein Sci 1*:1162-1172.

Kim PS, Baldwin RL. 1990. Intermediates in the folding reactions of small proteins. *Annu Rev Biochem 59*:631-660.

Kumar A, Ernst RR, Wüthrich K. 1980. A two-dimensional nuclear Overhauser enhancement (2D NOE) experiment for the elucidation of complete proton-proton cross relaxation networks in biological macromolecules. *Biochem Biophys Res Commun 96*:1-6.

Landt O, Grunert HP, Hahn U. 1990. A general method for rapid site-directed mutagenesis using the polymerase chain reaction. *Gene 96*:125-128.

Lin SH, Konishi Y, Denton ME, Scheraga HA. 1984. Influence of an extrinsic cross-link on the folding pathway of ribonuclease A. Conformational and thermodynamic analysis of cross-linked (lysine 7-lysine 41)-ribonuclease A. *Biochemistry 23*:5504-5512.

Lin SH, Konishi Y, Nall BT, Scheraga HA. 1985. Influence of an extrinsic cross-link on the folding pathway of ribonuclease A. Kinetics of folding-unfolding. *Biochemistry 24*:2680-2686.

Macura S, Ernst RR. 1980. Elucidation of cross relaxation in liquids by two-dimensional NMR spectroscopy. *Mol Phys 41*:95-117.

Marion D, Wüthrich K. 1983. Application of phase sensitive two-dimensional correlated spectroscopy (COSY) for measurements of ^{1}H-^{1}H spin-spin coupling constants in proteins. *Biochem Biophys Res Commun 113*: 967-974.

Martinez-Oyanedel J, Choe HW, Heinemann U, Saenger W. 1991. Ribonuclease T1 with free recognition and catalytic site: Crystal structure analysis at 1.5 Å resolution. *J Mol Biol 222*:335-352.

Matthews CR. 1993. Pathways of protein folding. *Annu Rev Biochem 62*:653–683.

Mayr LM. 1993. Untersuchungen zur Stabilität und Faltung von Ribonuklease T1 [dissertation]. Bayreuth, Germany: Universität Bayreuth.

Mayr LM, Kiefhaber T, Schmid FX. 1993a. Prolyl isomerizations as rate-determining steps in the folding of ribonuclease T1. *ACS Symp Ser 526*:142–155.

Mayr LM, Landt O, Hahn U, Schmid FX. 1993b. Stability and folding mechanism are strongly altered by the replacement of *cis* Pro 39 by an alanine residue. *J Mol Biol 231*:897–912.

Mayr LM, Schmid FX. 1993a. A purification method for labile variants of ribonuclease T1. *Protein Express Purif 4*:52–58.

Mayr LM, Schmid FX. 1993b. Kinetic models for unfolding and refolding of ribonuclease T1 with substitution of *cis*-proline 39 by alanine. *J Mol Biol 231*:913–926.

Mayr LM, Schmid FX. 1993c. Stabilization of a protein by guanidinium chloride. *Biochemistry 32*:7994–7998.

Mücke M, Schmid FX. 1992. Enzymatic catalysis of prolyl isomerization in an unfolding protein. *Biochemistry 31*:7848–7854.

Mullins LS, Pace CN, Raushel FM. 1993. Investigation of ribonuclease T1 folding intermediates by hydrogen/deuterium amide exchange–2D NMR spectroscopy. *Biochemistry 32*:6152–6156.

Neubert LA, Carmack M. 1974. Circular dichroism of disulfides with dihedral angles of 0, 30, and 60° in the 400–185 nm spectral region. *J Am Chem Soc 96*:943–945.

Oshima T, Uenishi N, Imahori K. 1976. Simple assay methods for ribonuclease T1, T2 and nuclease P1. *Anal Biochem 71*:632–634.

Pace CN. 1986. Determination and analysis of urea and guanidine hydrochloride denaturation curves. *Methods Enzymol 131*:266–280.

Pace CN. 1990. Conformational stability of globular proteins. *Trends Biochem Sci 15*:14–17.

Pace CN, Creighton TE. 1986. The disulphide folding pathway of ribonuclease T1. *J Mol Biol 188*:477–486.

Pace CN, Grimsley GR, Thomson JA, Barnett BJ. 1988. Conformational stability and activity of ribonuclease T1 with zero, one, and two intact disulfide bonds. *J Biol Chem 263*:11820–11825.

Poland DC, Scheraga HA. 1965. Statistical mechanics of non-covalent bonds in polyamino acids. VIII. Covalent loops in proteins. *Biopolymers 3*:379–399.

Radford SE, Dobson CM, Evans PA. 1992. The folding of hen lysozyme involves partially structured intermediates and multiple pathways. *Nature 358*:302–307.

Rance M, Sörensen OW, Bodenhausen G, Wagner G, Ernst RR, Wüthrich K. 1983. Improved spectral resolution in COSY ^{1}H NMR spectra of proteins via double quantum filtering. *Biochem Biophys Res Commun 117*:479–485.

Roder H, Elöve GA. 1993. Early stages in protein folding. In: Pain RH, ed. *Issues in protein folding*. Forthcoming.

Roder H, Elöve GA, Englander SW. 1988. Structural characterization of folding intermediates in cytochrome *c* by H-exchange labelling and proton NMR. *Nature 335*:700–704.

Santoro MM, Bolen DW. 1988. Unfolding free energy changes determined by the linear extrapolation method. 1. Unfolding of phenylmethanesulfonyl α-chymotrypsin using different denaturants. *Biochemistry 27*:8063–8068.

Schellman JA. 1955. The stability of hydrogen-bonded peptide structures in aqueous solution. *C R Trav Lab Carlsberg Ser Chim 29*:230–259.

Schönbrunner ER, Mayer S, Tropschug M, Fischer G, Takahashi N, Schmid FX. 1991. Catalysis of protein folding by cyclophilins from different species. *J Biol Chem 266*:3630–3635.

Segawa S, Kume K. 1986. Comparison between the unfolding rate and structural fluctuations in native lysozyme—Effects of denaturants, ligand binding, and intrachain cross-linking on hydrogen exchange and unfolding kinetics. *Biopolymers 25*:1981–1996.

Segawa S, Sugihara M. 1984. Characterization of the transition state of lysozyme unfolding. II. Effects of the intrachain crosslinking and the inhibitor binding on the transition state. *Biopolymers 23*:2489–2498.

Stassinopoulou CI, Wagner G, Wüthrich K. 1984. Two-dimensional ^{1}H NMR of two chemically modified analogs of the basic pancreatic trypsin inhibitor. *Eur J Biochem 145*:423–430.

States DJ, Creighton TE, Dobson CM, Karplus M. 1987. Conformations of intermediates in the folding of the pancreatic trypsin inhibitor. *J Mol Biol 195*:731–739.

Takahashi K, Uchida T, Egami F. 1970. Ribonuclease T1: Structure and function. *Adv Biophys 1*:53–98.

Tanford C. 1968. Protein denaturation. *Adv Protein Chem 23*:121–282.

Tidor B, Karplus M. 1993. The contribution of cross-links to protein stability: A normal mode analysis of the configurational entropy of the native state. *Proteins Struct Funct Genet 15*:71–79.

Udgaonkar JB, Baldwin RL. 1988. NMR evidence for an early framework intermediate on the folding pathway of ribonuclease A. *Nature 335*: 694–699.

van Mierlo CP, Darby NJ, Neuhaus D, Creighton TE. 1991. (14–38, 30–51) Double-disulphide intermediate in folding of bovine pancreatic trypsin inhibitor: A two-dimensional ^{1}H nuclear magnetic resonance study. *J Mol Biol 222*:353–371.

Wishart DS, Sykes BD, Richards FM. 1991. Relationship between nuclear magnetic resonance chemical shift and protein secondary structure. *J Mol Biol 222*:311–333.

Wüthrich K. 1986. *NMR of proteins and nucleic acids*. New York: Wiley-Interscience.

Zabinski M, Walz FG Jr. 1976. Subsites and catalytic mechanism of ribonuclease T1: Kinetic studies using GpC and GpU as substrates. *Arch Biochem Biophys 175*:558–564.